MILLING BIFURCATION AT EXTENDED AXIAL DEPTHS OF CUT

Andrew Honeycutt and Tony L. Schmitz
Mechanical Engineering and Engineering Sciences
University of North Carolina at Charlotte
Charlotte, NC

INTRODUCTION

In science and engineering fields, new discoveries are typically followed by a burst of follow-on research activity and corresponding publications. These discoveries tend to serve as a catalyst to the research community and often result in new insights, improved understanding of fundamental phenomena, and enhanced modeling capabilities. For machining, one such period of rapid progress began in the mid-19th century [1-3]. During this time, self-excited vibrations were first described using time-delay differential equations. The notion of "regeneration of waviness" was promoted as the feedback mechanism (time-delay term), where the previously cut surface combined with the instantaneous vibration state dictates the current chip thickness, force level, and corresponding vibration response. This work resulted in analytical algorithms that were used to produce the now well-known stability lobe diagram that separates the spindle speed-chip width domain into regions of stable and unstable behavior [4]; see Fig. 1.

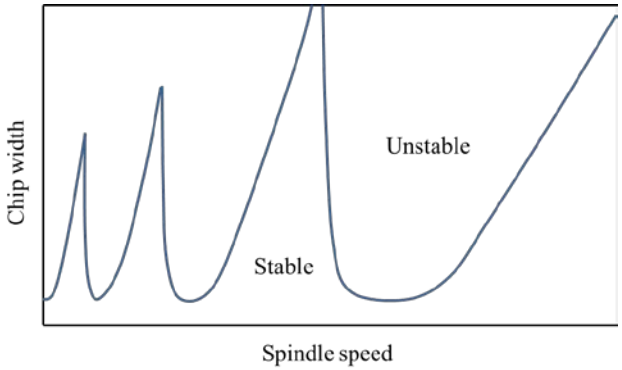

Figure 1. Example stability lobe diagram.

In 1998, a similar step forward in the understanding of machining behavior was realized. Davies *et al*. used once-per-revolution sampling to characterize the synchronicity of cutting tool motions (measured using a pair of orthogonal capacitance probes) with the tool rotation in milling [5]. This approach was an experimental modification of the Poincaré maps used to study state space orbits in nonlinear dynamics. They observed the traditional quasi-periodic chatter associated with the secondary (subcritical) Hopf, or Neimark-Sacker, bifurcation that can occur for systems described by periodic time-delay differential equations. This was an expected result and was observed as an elliptical cluster of once-per-revolution sampled points in the *x-y* measurement plane perpendicular to the endmill axis. This elliptical collection of points occurred because the chatter frequency was incommensurate with the tooth passing frequency and quasi-periodic behavior was obtained. However, they also recorded period-3 tool motion (i.e., motion that repeated with a period of three cutter revolutions) during partial radial immersion milling. This period-3 motion manifested itself as three distinct clusters of once-per-revolution sampled points in the *x-y* plane. They noted that this behavior was "inconsistent with existing theory" [5].

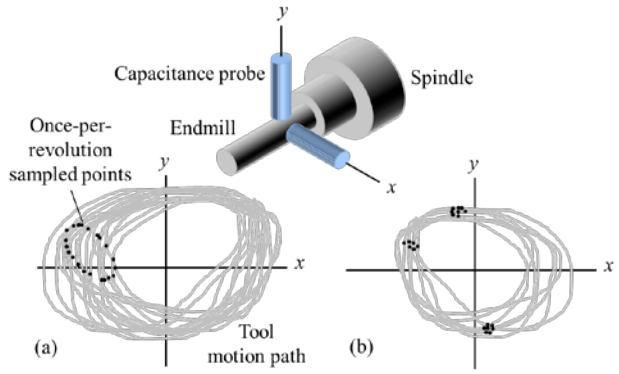

Figure 2. Once-per-revolution sampling of cutting tool motions (a) Hopf instability; (b) period-3 instability.

In this paper, bifurcation diagrams are used to study milling at extended axial depths of cut (beyond the stability limit). Initial results show that unexpected behavior occurs in the unstable region and that new milling strategies may be applied based on these results.

BIFURCATION DIAGRAMS

A bifurcation diagram enables the evolution of system behavior (e.g., tool motion) with a control variable of interest (such as axial depth of cut in milling) to be efficiently observed. The diagram uses the periodic sampling strategy to identify periodic (or aperiodic) responses over the selected range of the control variable. For milling, the tool motion in the feed, x, or y direction is sampled once per spindle revolution for

a given axial depth of cut (and fixed spindle speed). This produces a sequence of points over multiple cutter revolutions (see Fig. 2 for example). This collection of points is then truncated to remove the transient portion of the motion (typically the first few milliseconds).

For stable milling with motion that is periodic with the cutting force (i.e., only forced vibrations are present), these sampled points repeat each revolution because the cutting force and subsequent vibration response is periodic with the spindle rotation. The superposition of all these repeated points therefore gives a single point (or nearly so) on a bifurcation diagram of axial depth (horizontal axis) versus once-per-revolution sampled tool motion (vertical axis).

For a higher axial depth at the same spindle speed, secondary Hopf instability may occur and then the motion is quasi-periodic with tool rotation because the chatter frequency is (generally) incommensurate with the tooth passing frequency. In this case, the once-per-revolution sampled points do not repeat and they form a distribution (as shown in Fig. 2a). When plotted on the bifurcation diagram, this distribution appears as a vertical "spread" of points.

For period-2 instability, on the other hand, the motion repeats only once every other cycle (i.e., it is a sub-harmonic of the forcing frequency). In this case, the once-per-revolution sampled points alternate between two solutions. On the bifurcation diagram, the points appear in two distinct vertical locations (recall that the vertical axis is the sampled tool motion). For period-n instability, the sampled points appear at n vertical locations. The bifurcation diagram construction from results at multiple axial depths of cut for a selected spindle speed is depicted in Fig. 3.

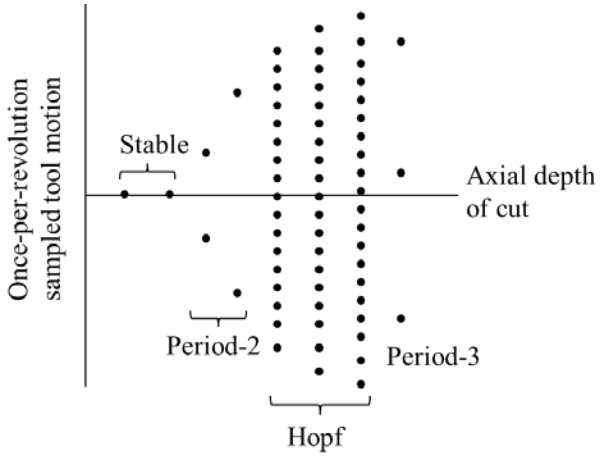

Figure 3. Description of stable/unstable behavior for a milling bifurcation diagram.

TIME-DOMAIN SIMULATION

Time-domain simulation entails the numerical solution of the governing equations of motion for milling in small time steps. It is well-suited to incorporating all the intricacies of milling dynamics, including the nonlinearity that occurs if the tooth leaves the cut due to large amplitude vibrations and complicated tool geometries (including runout, or different radii, of the cutter teeth, non-proportional teeth spacing, and variable helix). The simulation is based on the Regenerative Force, Dynamic Deflection Model described by Smith and Tlusty [6]. As opposed to stability lobe diagrams that provide a "global" picture of the stability behavior, time-domain simulation provides information regarding the "local" cutting force and vibration behavior (at the expense of computational efficiency) for the selected cutting conditions. The simulation proceeds as follows:

1. the instantaneous chip thickness is determined using the vibration of the current and previous teeth at the selected tooth angle
2. the cutting force is calculated
3. the force is used to find the new displacements
4. the tooth angle is incremented and the process is repeated. Modal parameters are used to describe the system dynamics in the x (feed) and y directions, where multiple degrees of freedom in each direction can be accommodated.

The instantaneous chip thickness depends on the nominal, tooth angle-dependent chip thickness, the current vibration in the direction normal to the surface, and the vibration of previous teeth at the same angle. The chip thickness can be expressed using the circular tool path approximation as $h(t) = f_t \sin\phi + n(t-\tau) - n(t)$, where f_t is the commanded feed per tooth, ϕ is the tooth angle, n is the normal direction, and τ is the tooth period. The tooth period is defined as $\tau = \frac{60}{\Omega N_t}$ (sec), where Ω is the spindle speed in rpm and N_t is the number of teeth. The vibration in the direction of the surface normal for the current tooth depends on the x and y vibrations as well as the tooth angle according to $n = x\sin\phi - y\cos\phi$.

For the simulation, the strategy is to divide the angle of the cut into a discrete number of steps. At each small time step, dt, the cutter angle is incremented by the corresponding small angle, $d\phi$. This approach enables convenient computation of the chip thickness for each simulation step because: 1) the possible teeth orientations are predefined; and 2) the surface created by the previous teeth at each angle may be stored. The cutter rotation $\phi = \frac{360}{SR}$ (deg)

depends on the selection of the number of steps per revolution, *SR*. The corresponding time step is $dt = \frac{60}{SR\,\Omega}$ (sec). A vector of angles is defined to represent the potential orientations of the teeth as the cutter is rotated through one revolution of the circular tool path, ϕ = *[0, dϕ, 2 dϕ, 3 dϕ, … , (SR – 1) dϕ].* The locations of the teeth within the cut are then defined by referencing entries in this vector.

In order to accommodate the helix angle for the tool's cutting edges, the tool may be sectioned into a number of axial slices. Each slice is treated as an individual straight tooth endmill, where the thickness of each slice is a small fraction, *db*, of the axial depth of cut, *b*. Each slice incorporates a distance delay $r\chi = db\tan\gamma$ relative to the prior slice (nearer the cutter free end), which becomes the angular delay between slices: $\chi = \frac{db\,tan\gamma}{r} = \frac{2db\,tan\gamma}{d}$ (rad) for the rotating endmill, where *d* is the endmill diameter and γ is the helix angle. In order to ensure that the angles for each axial slice match the predefined tooth angles, the delay angle between slices is $\chi = d\phi$. This places a constraint on the *db* value. By substituting *d*ϕ for χ and rearranging, the required slice width is $db = \frac{d\cdot d\phi}{2\tan\gamma}$. Using the time-domain simulation approach, the forces and displacements may be calculated. These results are then once-per-revolution sampled to generate the bifurcation diagrams.

RESULTS

As noted, the semi-discretization method was applied to predict Hopf and period-2 bifurcation. These predictions were verified experimentally and were reported in [7]. The up milling tests were completed using an 8 mm diameter endmill (mounted in a shrink fit tool holder) with one cutting edge, a 45 deg helix angle, and a 96 mm overhang. The radial depth of cut was 0.4 mm to provide highly interrupted cutting conditions. The aluminum workpiece and tool combination yielded a force model with a specific cutting force of 644 MPa and 69.7 deg force angle.

The long, slender tool exhibited a single dominant bending mode. The modal parameters for the x (feed) and y directions are provided in Table 1.

Table 1: Modal parameters obtained from impact testing.

Direction	Natural frequency (Hz)	Damping ratio (-)	Stiffness (N/m)
x	721	0.009	4.1×10^5
y	721	0.009	4.1×10^5

The stability diagram obtained from the semi-discretization method is plotted in Fig. 4. Lines are added that depict the spindle speeds that were used for the extended milling bifurcation diagrams. The modifier "extended" is used to emphasize that axial depths well beyond the predicted stability limit were used.

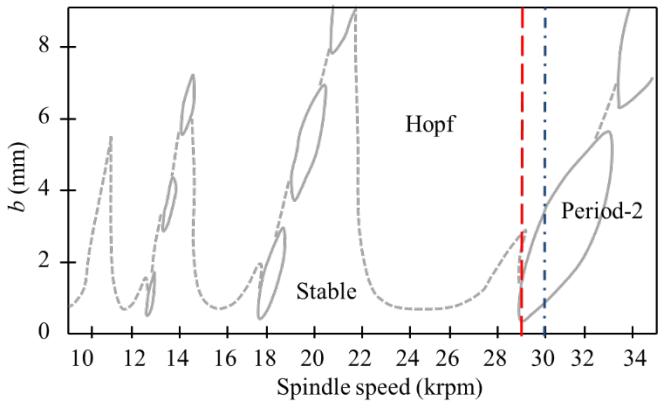

Figure 4. Stability lobe diagram with stable and unstable (Hopf and period-2) zones (from [7]). Test speeds for the bifurcation diagrams are identified: (dashed line) 29000 rpm; (dash-dot line) 30000 rpm.

In Fig. 4 it is observed that the 29000 rpm (dashed) line predicts stable behavior up to an axial depth of 0.3 mm. Period-2 instability then occurs up to an axial depth of 2 mm. Stable performance is again predicted until 2.5 mm. Hopf instability then occurs for higher depths of cut.

The corresponding bifurcation diagram is presented in Fig. 5. The vertical axis represents the once-per-revolution sampled x-direction tool motions, while the horizontal axis is the axial depth of cut. The transition from stable to period-2 motion occurs at 0.26 mm; the period-2 instability persists with increasing amplitude until an axial depth of 2.1 mm. Stable operation is again obtained at 2.1 mm and is maintained until 2.4 mm. Hopf instability then occurs. The second stable zone validates the closed islands of stability depicted in Figs. 3 and 5. Regions of period-7 (3.38 mm to 3.54 mm) and period-5 (4.48 mm to 4.7 mm) instability are also observed. This behavior is not predicted by existing milling stability

theory and, to the authors' knowledge, has not been previously presented in the literature.

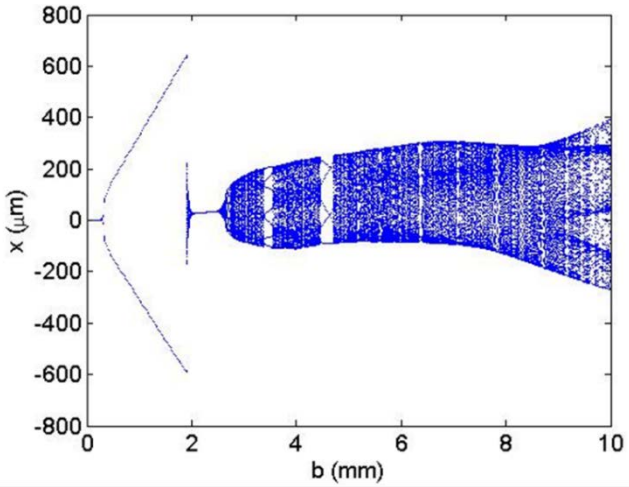

Figure 5. Extended milling bifurcation diagram (29000 rpm).

A bifurcation diagram was also produced for 30000 rpm (dash-dot line in Fig. 4). In Fig. 6, a transition from stable to period-2 motion is seen at 0.68 mm. The period-2 behavior persists to an axial depth of b = 1.26 mm where combination period-2 and quasi-periodic motion occurs. This is exhibited by the two separate vertical spreads in points. At 1.88 mm, the motion changes to quasi-periodic only and a single, vertical distribution of once-per-revolution sampled points is seen.

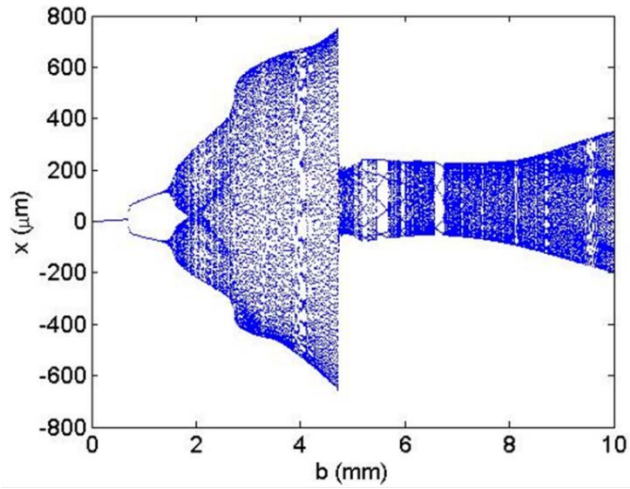

Figure 6. Extended milling bifurcation diagram (30000 rpm).

The significance of the extended range bifurcation diagram is seen at an axial depth of 4.76 mm. A dramatic amplitude reduction is observed at this depth, even though the cut remains unstable. This reduced amplitude at a high axial depth could provide acceptable cutting conditions, while offering a high material removal rate. Additionally, period-7 instability is predicted in the range from b = 5.48 mm to 5.66 mm. As noted, milling stability theory does not predict this behavior. These results call for additional analysis and experiments to better understand the predicted behavior.

These results demonstrate that the extended milling bifurcation diagram is a powerful tool to enable a detailed view of unstable behavior and elicit an improved understanding of milling dynamics. It is expected that this new understanding will lead to new milling strategies that improve productivity.

REFERENCES

[1] Arnold RN (1946) The mechanism of tool vibration in the cutting of steel. Proceedings of the Institute of Mechanical Engineers, 154.

[2] Tobias SA, Fishwick W (1958) The chatter of lathe tools under orthogonal cutting conditions. Transactions of the ASME, 80:1079-1088.

[3] Tlusty J, Polacek M (1963) The stability of machine tools against self-excited vibrations in machining. Proceedings of the ASME International Research in Production Engineering Conference, Pittsburgh, PA, 465-474.

[4] Schmitz T, Smith S (2009) Machining Dynamics: Frequency Response to Improved Productivity. Springer, New York, NY.

[5] Davies MA, Dutterer BS, Pratt JR, Schaut AJ (1998) On the dynamics of high-speed milling with long, slender endmills. Annals of the CIRP 47(1):55-60.

[6] Smith, K.S. and Tlusty, J., 1991, An overview of modeling and simulation of the milling process, Journal of Engineering for Industry, 113: 169-175.

[7] Govekar, E., Gradišek, J., Kalveram, M., Insperger, T., Weinert, K., Stepan, G., and Grabec, I., 2005, On stability and dynamics of milling at small radial immersion, Annals of the CIRP, 54/1: 357-362.